

Fingering Instability Accelerates Population Growth of a Proliferating Cell Collective

Yiyang Ye (叶毅扬)¹ and Jie Lin (林杰)^{1,2,*}

¹Center for Quantitative Biology, Peking University, Beijing, China

²Peking-Tsinghua Center for Life Sciences, Peking University, Beijing, China



(Received 20 June 2023; accepted 17 November 2023; published 3 January 2024)

During the growth of a cell collective, such as proliferating microbial colonies and epithelial tissues, the local cell growth increases the local pressure, which in turn suppresses cell growth. How this pressure-growth coupling affects the growth of a cell collective remains unclear. Here, we answer this question using a continuum model of a cell collective. We find that a fast-growing leading front and a slow-growing interior of the cell collective emerge due to the pressure-dependent growth rate. The leading front can exhibit fingering instability, and we confirm the predicted instability criteria numerically with the leading front explicitly simulated. Intriguingly, we find that fingering instability is not only a consequence of local cell growth but also enhances the entire population's growth rate as positive feedback. Our work unveils the fitness advantage of fingering formation and suggests that the ability to form protrusions can be evolutionarily selected.

DOI: 10.1103/PhysRevLett.132.018402

Summary for biologists.—Proliferating cell collectives, such as tumors and microbial colonies, are ubiquitous in biology. For the cells at the interior of the collective to grow, they need to push the cells at the outside, which generates a higher pressure at the interior. Meanwhile, experiments showed that high pressure reduces cancer cell proliferation and drives apoptosis. In microorganisms, several experiments have suggested that high pressure may trigger a glass transition (an amorphous liquid becomes solid) of the cytoplasm, above which the mobility of biomolecules virtually stops. This crowding effect slows down the intracellular reaction rates and the growth rate. How does the interconnected feedback between growth and pressure affect the proliferation of cell collectives? In this work, we aim to answer this question using a physical approach.

During our research, we realized that the instability of the cell collective interface plays a key role, which can occur during epithelial spreading, biofilm pattern formation, and embryonic development. Knowledge from physics tells us that the flat interface between a cell collective and the environment can be susceptible to mechanical instability and develop finger-shaped morphologies. Instability can be triggered by purely physical mechanisms, such as the Saffman-Taylor instability. This type of instability triggers the fingering formation of the interface between two fluids with different friction coefficients against the substrate in two dimensions. In our work, we extend the traditional Saffman-Taylor instability to actively proliferating cell collectives. Interestingly, we find that interface instability of a proliferating cell collective can be triggered not only by its low friction coefficient against the substrate but also by its active growth. When a protrusion of

the interface occurs, the pressure and velocity inside the protrusion surpass the outside passive fluid, leading to further enlargement of the protrusion.

Our key finding is that protrusions resulting from interface instability are not merely consequences of active cellular growth; they also alleviate the pressure, boost local growth rates in the protrusions, and consequently speed up the population growth rate of the entire cell collective. Our findings unveil the evolutionary significance of protrusion formation. Selective pressures on faster growth may affect the physical properties of cells so that protrusion formation is more prone to occur. For example, cells may express more lubricant to lower the friction coefficient or modify the surface properties to reduce the surface tension. Another related example is the epithelial-mesenchymal transition in cancer, where the tissue changes from an epithelium to a mesenchymal phenotype with facilitated cell motility.

Introduction.—Growing cell collectives are ubiquitous, e.g., developing microbial colonies, wound healing, and tumor growth [1–6]. During the growth, the local pressure and single-cell growth rate can be spatially heterogeneous across the cell collective. For example, a growing cell collective often displays a leading front underneath which cells actively grow and divide, followed by a crowded interior where cells grow slowly [4,5,7–12]. Experiments demonstrated that the low growth rates of interior cells could result from high pressure because a high confining pressure can slow or even completely halt the cell cycle progression [13–17]. On the other hand, the pressure itself is generated by active cell growth as a high cell density due to cell division inevitably increases the local pressure. Therefore, the temporal and spatial patterns of pressure and

local growth rate are intimately coupled. However, how the interconnection between pressure and cell growth affects the growth of a cell collective is not understood. In the meantime, the leading front of the cell collective often exhibits protrusions due to fingering instability [1,18–22]. While the conditions of fingering instability and morphologies of interfaces have been widely studied in different contexts [9,23–34], it is unclear whether the protrusion can speed up the invasion of a cell collective to its environment relative to a collective without protrusions.

This work combines theoretical analysis and computer simulations to study a continuum model of a cell collective in two dimensions. We show that a fast-growing leading front and a slow-growing interior of the cell collective emerge as an outcome of the pressure-dependent growth rate. The leading front can exhibit fingering instability due to active cellular growth and the different friction coefficients between the cell collective and passive fluid. To corroborate with our theory, we simulate a numerical model in which the interface separating the cell collective and the environment is explicitly simulated. Surprisingly, the formation of protrusions due to fingering instability enhances the population growth rate by relaxing the pressure and increasing the local growth rate relative to a collective without protrusions under the same parameters. We show that the population growth rate of the collective increases as the surface tension constant decreases. Thus, our work provides a minimal model of a proliferating cell that accounts for the interplay between pressure and growth rate, as well as a quantitative measure for the fitness advantage of fingering instability.

The cell collective growth model.—We study the growth of a two-dimensional cell collective surrounded by a passive fluid (Fig. 1). The system we consider is half of a cell collective expanding in both directions of x . Owing to the symmetry with respect to $x = 0$, only the cell collective within $0 \leq x \leq L$ is considered, where L is the total length in the x direction. The boundary condition is periodic in the y direction with length L_y . In this section, we ignore the

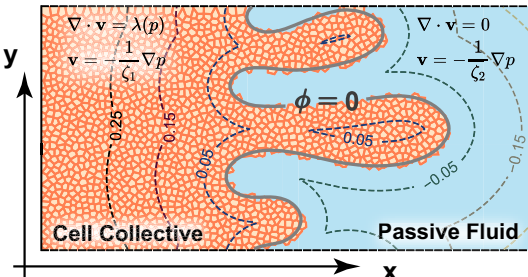


FIG. 1. A schematic of a cell collective growing in the x direction. In the continuum model, the velocity field under active cell growth is described as Eqs. (1) and (2). In numerical simulations, we use a level-set function ϕ to distinguish the cell collective from the passive fluid, where $\phi = 0$ corresponds to the interface.

possibility of fingering instability, and the flat interface separating the cell collective and the passive fluid is labeled by its x coordinate x_I . The velocity field satisfies Darcy's law,

$$\mathbf{v} = -\nabla p/\zeta_1, \quad \nabla \cdot \mathbf{v} = \lambda(p) \quad \text{for } x < x_I, \quad (1)$$

$$\mathbf{v} = -\nabla p/\zeta_2, \quad \nabla \cdot \mathbf{v} = 0 \quad \text{for } x \geq x_I, \quad (2)$$

where ζ_1 and ζ_2 are the friction coefficients of the cell collective and the passive fluid over the substrate, which can depend on the substrate stiffness [35] and the cell-substrate ligand properties [36]. We set the pressure at the rightmost side of the system to be zero, $p|_{x=L} = 0$, without losing generality since only the pressure gradient matters in Eqs. (1) and (2). Since the velocity vanishes at $x = 0$ by symmetry, the pressure gradient at $x = 0$ is zero, $\partial p(x)/\partial x|_{x=0} = 0$. Owing to the overdamped nature of the dynamics described by Eqs. (1) and (2), given an interface morphology, the pressure and velocity fields are fully determined.

In using Darcy's law to describe the dynamics of the velocity field, we have assumed that the dissipation due to internal viscosity is much smaller than that due to friction [37,38], which is valid for systems with their sizes above the hydrodynamic screening length, which is around 0.5 mm for epithelial tissues [5,31]. We have also neglected the elastic property of the cell collective because the timescale of the population growth, typically around hours, is much longer than the protein turnover times in cell-cell junctions [39]. For simplicity, we assume that both the cell collective and the surrounding fluid are incompressible. Therefore, the divergence of the velocity field located inside and outside the cell collective is equal to the local growth rate $\lambda(p)$ and 0, respectively.

Given the pressure dependence of the growth rate, the analytical form of the pressure can be determined, assuming a homogeneity along the y direction. In our model, we set the growth rate to be a linear function of the pressure to gain analytical insights: $\lambda = \lambda_0(1 - p/p_c)$ where p_c is the threshold pressure (also called homeostatic pressure), above which the growth rate can be negative [30,40–42]. In our model, however, the growth rate must be positive everywhere for a proliferating cell collective (see the detailed proof in the Supplemental Material [43]), in agreement with our numerical simulations, as we show later. In the Supplemental Material [43], we also extend our model to the case of compressible cell collectives and find that our main conclusions from the incompressible model also apply to the compressible case even if the bulk modulus of the collective is comparable to the threshold pressure p_c .

In contrast to a bumpy interface where surface tension γ causes a pressure jump across it, a flat interface maintains continuity in both velocity and pressure fields.

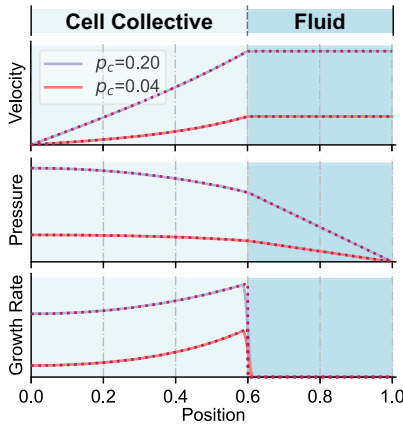


FIG. 2. Theoretical predictions (dashed lines) in the absence of fingering instability are compared with numerical simulations (solid lines) at two threshold pressures p_c .

Together with the boundary conditions $p|_{x=L} = 0$ and $\partial p(x)/\partial x|_{x=0} = 0$, the pressure profile is exactly solvable:

$$p = p_c - A \cosh\left(\frac{x}{x_c}\right) \quad \text{for } x < x_I, \quad (3)$$

$$p = v_I(L - x) \quad \text{for } x \geq x_I. \quad (4)$$

Here, A is a constant, and v_I is the interface velocity (see detailed expressions in the Supplemental Material [43]). $x_c \equiv \sqrt{p_c/\zeta_1 \lambda_0}$ is the characteristic length scale of the pressure fields (Fig. 2). Given Eq. (3), the local growth rate becomes

$$\lambda = \lambda_0 \frac{A}{p_c} \cosh\left(\frac{x}{x_c}\right), \quad (5)$$

which exhibits a slow-growing region in the collective interior with the characteristic width x_c (Fig. 2). In this work, we nondimensionalize our model with length unit L , time unit $1/\lambda_0$, pressure unit $\lambda_0 \zeta_2 L^2$, and surface tension unit $\lambda_0 \zeta_2 L^3$. We define the ratio of friction coefficients $\alpha \equiv \zeta_1/\zeta_2$. In the following, all variables are dimensionless unless specifically mentioned. We compute the advancing speed of the flat interface $v_I(x_I)$, and find that the cell collective grows faster when the friction coefficient of the cell collective becomes smaller (Fig. S1).

Criteria of fingering instability.—In the case of traditional fingering instability, i.e., the Saffman-Taylor instability, the moving interface separating two fluids is pushed by a constant velocity from the infinity [48]. Therefore, only the pressure gradient exhibits a jump across the interface. For a growing cell collective, the moving interface is pushed by active cell growth. Because of the finite growth rate, the velocity gradient also exhibits a jump across the interface (Fig. 2). To test whether both two gradient jumps contribute to interface instability, we

introduce a periodic perturbation $\xi_k(t) \exp(iky)$ to a flat interface and derive the time dependence of the perturbation amplitude (Supplemental Material [43]),

$$\frac{\dot{\xi}_k}{\xi_k} = \frac{k v_I(1 - \alpha) - \gamma k^3 + \alpha \frac{k}{\tilde{k}} \lambda^{(0)}(x_I) \coth(\tilde{k} x_I)}{\alpha \frac{k}{\tilde{k}} \coth(\tilde{k} x_I) + \frac{\exp(2k) - \exp(2k x_I)}{\exp(2k) + \exp(2k x_I)}}. \quad (6)$$

Here, $\lambda^{(0)}(x_I)$ is the local growth rate at the leading front in the absence of instability, and $\tilde{k} = \sqrt{k^2 + 1/x_c^2}$. For each flat interface at a given position x_I , the perturbation is unstable within a certain range of wave number [Fig. 3(a)], and we define k_c as the critical wave number below which the interface is unstable against perturbation.

When the friction coefficient of the cell collective is smaller than the passive fluid, the pressure gradients are different across the interface, corresponding to the first term in the numerator of Eq. (6). The different velocity gradients across the interface are due to active cell growth, corresponding to the third term in the numerator of Eq. (6). Because $k \coth(\tilde{k} x_I)/\tilde{k} \rightarrow 1$ as $k \rightarrow +\infty$, one can always find a k so that $\alpha \lambda^{(0)}(x_I) k \coth(\tilde{k} x_I)/\tilde{k} \ll k v_I(1 - \alpha)$. Thus, the instability is mainly driven by the pressure gradient difference for a small surface tension constant $\gamma \ll 1$. We plot the phase boundaries from the full prediction (solid line) and from the prediction after neglecting the velocity gradient, which is $k_c = \sqrt{v_I(1 - \alpha)/\gamma}$ (dashed line) in the phase diagram of interface stability [Fig. 3(c)]. Agreement in these two curves supports our prediction that instability is mainly driven by a pressure gradient difference for small γ .

Interestingly, in the case of an proliferating cell collective, instability can be driven by active growth alone [29]. In the following, we discuss the case of $\alpha = 1$, where the interface instability is purely driven by active growth, and focus on a particular asymptotic regime, $x_I \gg 1/k_c \gg x_c$. In this regime, the small threshold pressure p_c imposes a strong constraint on the growth rate, and most cell growth occurs near the interface. The growth rate at the interface satisfies $\lambda_I = x_c/(1 - x_I)$, with $\coth(\tilde{k}_c x_I) \approx 1$, and $\tilde{k}_c \approx 1/x_c$ (see the Supplemental Material [43]). Therefore, the critical wave number satisfies $k_c \approx x_c/\sqrt{\gamma(1 - x_I)}$, which matches the full prediction (solid line) pretty well [Fig. 3(d)]. Discussions of another asymptotic regime for $\alpha = 1$ are included in the Supplemental Material [43], where the value of p_c has a negligible effect on the growth rate (Fig. S2). We also include discussions for the case of $\alpha > 1$ wherein active growth can induce fingering instability by exceeding the stabilizing effect from the surface tension and the pressure gradient (see the Supplemental Material [43] and Fig. S3).

Simulations of the cell collective growth.—We simulate the growth of a cell collective by explicitly simulating the interface using the level set method [44–46]. The key idea is to define a level set function $\phi(\mathbf{x})$ as the signed distance

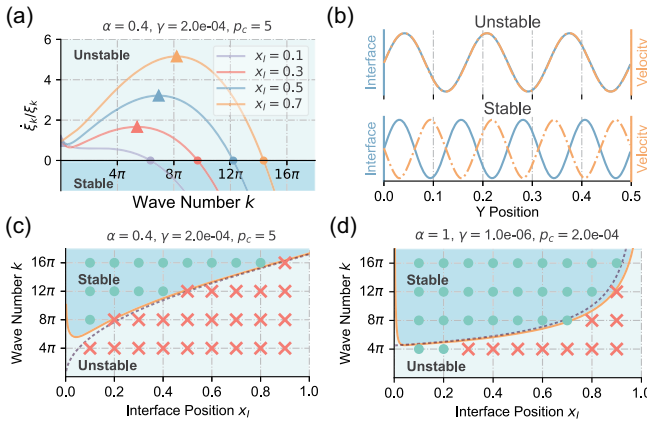


FIG. 3. Conditions of fingering instability and numerical verifications. (a) In the linear instability analysis, instability occurs when $\dot{\xi}_k/\xi_k > 0$. Circles mark the critical wave numbers where $\dot{\xi}_k/\xi_k = 0$. Triangles mark the wave numbers with the maximum $\dot{\xi}_k/\xi_k$. (b) A sinusoidal perturbation is applied to the flat interface in the numerical simulations. A negative correlation between the perturbation and the interface velocity change leads to a stable interface and vice versa for an unstable interface. The unstable example corresponds to $x_I = 0.7$, $k = 12\pi$ in (c), and the stable example corresponds to $x_I = 0.7$, $k = 16\pi$ in (c). (c), (d) Phase diagram for the interface stability. The solid line represents the theoretical result of the linear instability analysis. According to simulations, stable interfaces are marked as green dots, while unstable ones are marked as red crosses. In (c), the interface instability is dominated by the pressure gradient difference across the interface, and the dashed line is the prediction merely considering the effects of the pressure gradient. In (d), the interface instability is purely induced by active cell growth since $\alpha \equiv \zeta_1/\zeta_2 = 1$. The dashed line represents the asymptotic result in the limit $x_I \gg 1/k_c \gg x_c$.

to the interface satisfying the constraint $|\nabla\phi| = 1$. In our notation, positive ϕ represents the cell collective, while negative ϕ is for the passive fluid. The interface is the contour line with $\phi = 0$ (Fig. 1).

Equations (1) and (2) are unified using the following equation:

$$\nabla p + \zeta(\phi)\mathbf{v} - \gamma\kappa\delta(\phi; \epsilon)\mathbf{n} = 0. \quad (7)$$

Here, $\mathbf{n} = -\nabla\phi$ is the unit vector normal to the interface, and $\kappa = \nabla \cdot \mathbf{n}$ is the local curvature of the interface. Therefore, $\gamma\kappa\delta(\phi; \epsilon)\mathbf{n}$ in Eq. (7) corresponds to the surface tension. Different friction coefficients between the two phases are characterized by a Heaviside function with a finite width 2ϵ , $\zeta(\phi) = \zeta_2 + (\zeta_1 - \zeta_2)H(\phi; \epsilon)$. Its corresponding delta function is defined as $\delta(\phi; \epsilon) \equiv dH(\phi; \epsilon)/d\phi$. As the interface moves, ϕ is convected with the velocity field to capture the movement of the interface, $\dot{\phi} + \mathbf{v} \cdot \nabla\phi = 0$ (see simulation details in the Supplemental Material [43]). The simulated pressure and velocity profiles agree well with the theoretical predictions (Fig. 2).

Fingering instability accelerates population growth.— We verify the instability criteria numerically by adding a prescribed perturbation with wave vector k along the y direction. The perturbation grows if the original perturbation and its following change have a zero phase shift and shrinks if the phase shift is π [Fig. 3(b)]. We find that Eq. (6) accurately predicts whether the interface is stable or not [Figs. 3(c) and 3(d)].

We compare two growing cell collectives with identical α and p_c but different surface tension constants γ to unveil the evolutionary advantage due to fingering instability. In the cell collective with a small γ , we apply a small perturbation to the initial flat interface to trigger fingering instability [Eq. (S31) and Movie S1 in the Supplemental Material [43]]. In the other collective with a large γ , we do not add noise to ensure the interface is flat throughout the simulation [Figs. 4(a) and 4(b), and Movie S2]. Interestingly, after the same duration since the initial condition, the cell collective exhibiting instability appears to grow faster. In particular, the local growth rate and velocity magnitude are much higher in the fingers than in the bulk [Fig. 4(c)]. Furthermore, the bulk pressure of the unstable cell collective is significantly lower than the stable one [Figs. 4(b) and 4(d)]. These results suggest that the protrusions can relax the pressure and increase the local growth rate. In the cases of small surface tension constants, we can even observe bubbles disconnected from the bulk (Fig. S7).

To quantify the advantage of instability, we compute the population growth rate, defined as $\Lambda_p = (dV_{\text{cell}}/dt)/V_{\text{cell}}$ where V_{cell} is the volume of the cell collective. According to the length unit we use for normalization, the system size in the x direction is 1 and 0.5 in the y direction; therefore, the maximum value of V_{cell} is 0.5. According to Eq. (6), a smaller surface tension constant triggers the instability at an earlier stage, resulting in more pronounced protrusions. Therefore, we expect cell collectives with smaller γ to grow faster. Indeed, the population growth rate increases as the surface tension constant decreases given the same total volume [Figs. 4(e) and 4(g)]. Meanwhile, a stable cell collective always exhibits a smaller population growth rate than the unstable one [the dot-dashed line in Fig. 4(e)].

We find that the interface velocity is often a convex function of the interface position for a stable collective (see Fig. S1 and the proof in the Supplemental Material [43]), which provides an intuitive way to understand the enhancement of the population growth rate. We compare two cell collectives: one with a bumpy interface $x_I(y)$ and one with a flat interface at the position \bar{x}_I . They have the same total volume so that $V_{\text{cell}} = \int_0^{L_y} x_I(y) dy = \bar{x}_I L_y = \bar{V}_{\text{cell}}$. Using Jensen's inequality, we find $d\bar{V}_{\text{cell}}/dt = L_y v_I(\bar{x}_I) \leq \int_0^{L_y} v_I[x_I(y)] dy \approx dV_{\text{cell}}/dt$. Here, we have approximated the advancing speed at each point on a bumpy interface to be that of a flat interface at the same position, which is valid

if the wavelength of the bumpy interface is long enough. Therefore, the cell collective with a bumpy interface has a larger population growth rate. As the protrusions grow, they further relax the pressure and enhance the population growth rate.

Given the linear pressure dependence of the local growth rate, the population growth rate turns out to be a linear function of the average pressure inside the collective, $\Lambda_p = \lambda_0(1 - \langle p \rangle / p_c)$. Two factors determine the average pressure: the amount of passive fluid pushed by the cell collective and the speed at which the passive fluid is pushed. With a smaller cell collective, a larger amount of passive fluid is being pushed, but at a lower speed, whereas for a large cell collective, a smaller amount of passive fluid is being pushed at a higher speed. These two counter factors result in a nonmonotonic curve of Λ_p vs V_{cell} [Fig. 4(e)]. In the presence of fingering instability, Λ_p is a function of both the relative friction coefficient α and surface tension constant γ [Fig. 4(g)], while in the absence of instability, Λ_p is only a function of α (Fig. S8).

We speculate that the acceleration of population growth due to the protrusion formation results from the pressure-growth coupling. To confirm this, we also simulate a modified model in which the growth rate is strictly constant ($\lambda = \text{const}$) and find that, in this case, the population growth rate is always equal to λ regardless of the surface tension constant and the morphologies of the cell collective [Figs. 4(f) and S9].

Discussions.—In this Letter, we demonstrate that fingering instability can relieve the pressure confinement on cell growth and accelerate the collective growth. Our work suggests that selection pressures on the formation of protrusions may affect the physical properties of cells. For example, the cell surface can be more hydrophilic in an aqueous environment to reduce the surface tension constant. Meanwhile, significant fingering instability may also be suppressed during evolution because it might lead to a breakup of the cell collective, which can impair the ability of the population to sense gradients of stimuli collectively [49].

In Ref. [30], the authors studied the stability of an interface separating two proliferating tissues with different homeostatic pressures and active motility forces. They demonstrated that the motility force can also lead to instability, and mechanical feedback can help preserve reproducibility at the tissue scale when subjected to cell-level stochasticity. In this work, we go beyond the linear analysis and directly simulate a proliferating cell collective with a protruding interface, which allows us to unveil the fitness advantage of fingering instability. It will be interesting to extend our results by incorporating more biological complexities into our model, such as internal viscosity, active motility force [30,31], activity at interface [50], nutrient or chemoattractant consumption [49,51], and leader-follower cell interaction [52].

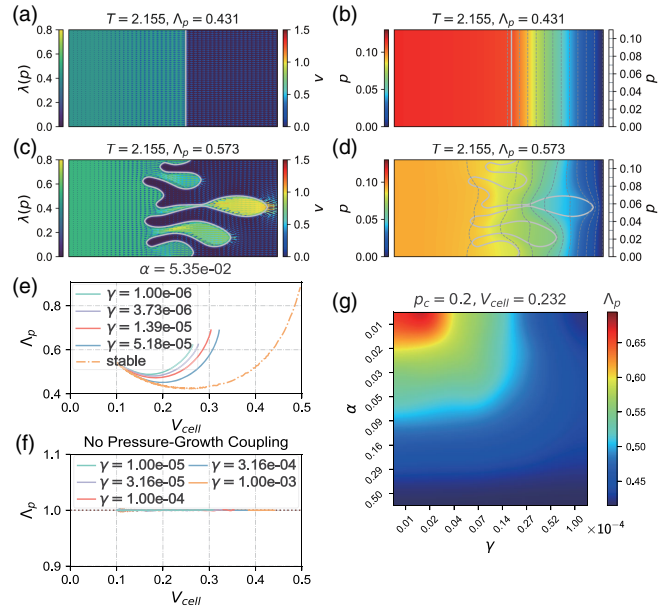


FIG. 4. Fingering instability accelerates population growth. (a) The local growth rate of a cell collective at a specific time, free of instability, is displayed with a color bar on the left. The arrows represent the velocity field, and its magnitude is displayed in the color bar on the right. Here, $\alpha = 9.35 \times 10^{-2}$, $\gamma = 1 \times 10^{-3}$. The interface is highlighted as the gray curve. (b) The pressure pattern of the same simulation as (a). The contour lines of the pressure field are shown with the pressure values on the right. The pressure value decreases from left to right. (c) In contrast to (a), we use a small $\gamma = 3.73 \times 10^{-6}$ and apply a perturbation to the initial flat interface so that the cell collective exhibits fingering instability. In this case, cells in the fingers have higher growth rates and larger velocity magnitudes than in the bulk. (d) The pressure pattern of the same simulation as (c), which is significantly lower than the case without instability, as shown in (a). (e) The population growth rate of the cell collective Λ_p as a function of the current volume V_{cell} given different surface tension constants. The curves stop when any part of the collective reaches the boundary in simulations. (f) The population growth rate of a cell collective without pressure-growth coupling does not depend on γ and is always equal to the local cell growth rate $\Lambda_p = 1$. (g) Heat map of the population growth rate Λ_p at a given total cell volume $V_{\text{cell}} = 0.232$ as a function of α and γ .

We propose that our model predictions are particularly relevant for expanding bacterial colonies and epithelial tissues surrounded by a viscous medium. To trigger a more significant instability, one can lower the friction coefficient of the cell collective, e.g., by the lubricant excreted by bacteria [53] or by modifying the adhesion ligands of epithelial cells through genetic or biochemical approaches [54,55]. Replacing the viscous medium with nongrowing or slow-growing cells is also possible, as previous experiments suggested that the friction coefficient can increase after cell death [56]. We remark that our conclusions regarding the enhancement of population growth by

instability are valid even if the friction coefficient of the cell collective is larger than that of the passive fluid (Fig. S10). It will be interesting to test our theories with experimental data quantitatively in the future, which has been done for other types of instability in epithelial tissues [21].

We thank Lingyu Meng and Sheng Mao for helpful discussions about this work. This work was supported by the National Key Research and Development Program of China (Grant No. 2021YFF1200500) and grants from Peking-Tsinghua Center for Life Sciences.

*Corresponding author: linjie@pku.edu.cn

- [1] M. Poujade, E. Grasland-Mongrain, A. Hertzog, J. Jouanneau, P. Chavrier, B. Ladoux, A. Buguin, and P. Silberzan, Collective migration of an epithelial monolayer in response to a model wound, *Proc. Natl. Acad. Sci. U.S.A.* **104**, 15988 (2007).
- [2] P. Friedl and D. Gilmour, Collective cell migration in morphogenesis, regeneration and cancer, *Nat. Rev. Mol. Cell Biol.* **10**, 445 (2009).
- [3] T. Zulueta-Coarasa and R. Fernandez-Gonzalez, Dynamic force patterns promote collective cell movements during embryonic wound repair, *Nat. Phys.* **14**, 750 (2018).
- [4] L. Xiong, Y. Cao, R. Cooper, W.-J. Rappel, J. Hasty, and L. Tsimring, Flower-like patterns in multi-species bacterial colonies, *eLife* **9**, e48885 (2020).
- [5] R. Alert and X. Trepat, Physical models of collective cell migration, *Annu. Rev. Condens. Matter Phys.* **11**, 77 (2020).
- [6] O. Hallatschek, S. S. Datta, K. Drescher, J. Dunkel, J. Elgeti, B. Waclaw, and N. S. Wingreen, Proliferating active matter, *Nat. Rev. Phys.* **5**, 407 (2023).
- [7] F. Montel, M. Delarue, J. Elgeti, L. Malaquin, M. Basan, T. Risler, B. Cabane, D. Vignjevic, J. Prost, G. Cappello, and J.-F. Joanny, Stress clamp experiments on multicellular tumor spheroids, *Phys. Rev. Lett.* **107**, 188102 (2011).
- [8] X. Serra-Picamal, V. Conte, R. Vincent, E. Anon, D. T. Tambe, E. Bazellieres, J. P. Butler, J. J. Fredberg, and X. Trepat, Mechanical waves during tissue expansion, *Nat. Phys.* **8**, 628 (2012).
- [9] N. Podewitz, F. Jülicher, G. Gompper, and J. Elgeti, Interface dynamics of competing tissues, *New J. Phys.* **18**, 083020 (2016).
- [10] A. N. Malmi-Kakkada, X. Li, H. S. Samanta, S. Sinha, and D. Thirumalai, Cell growth rate dictates the onset of glass to fluidlike transition and long time superdiffusion in an evolving cell colony, *Phys. Rev. X* **8**, 021025 (2018).
- [11] A. Saraswathibhatla, E. E. Galles, and J. Notbohm, Spatio-temporal force and motion in collective cell migration, *Sci. Data* **7**, 197 (2020).
- [12] J. Li, S. K. Schnyder, M. S. Turner, and R. Yamamoto, Role of the cell cycle in collective cell dynamics, *Phys. Rev. X* **11**, 031025 (2021).
- [13] G. Helmlinger, P. Netti, H. Lichtenbeld, R. Melder, and R. Jain, Solid stress inhibits the growth of multicellular tumor spheroids, *Nat. Biotechnol.* **15**, 778 (1997).
- [14] K. Alessandri, B. R. Sarangi, V. V. Gurchenkov, B. Sinha, T. R. Kießling, L. Fetler, F. Rico, S. Scheuring, C. Lamaze, A. Simon *et al.*, Cellular capsules as a tool for multicellular spheroid production and for investigating the mechanics of tumor progression *in vitro*, *Proc. Natl. Acad. Sci. U.S.A.* **110**, 14843 (2013).
- [15] M. Delarue, J. Hartung, C. F. Schreck, P. Gniewek, L. Hu, S. Herminghaus, and O. Hallatschek, Self-driven jamming in growing microbial populations, *Nat. Phys.* **12**, 762 (2016).
- [16] I. F. Rizzuti, P. Mascheroni, S. Arcucci, Z. Ben-Mérim, A. Prunet, C. Barentin, C. Rivière, H. Delanoë-Ayari, H. Hatzikirou, J. Guillermet-Guibert, and M. Delarue, Mechanical control of cell proliferation increases resistance to chemotherapeutic agents, *Phys. Rev. Lett.* **125**, 128103 (2020).
- [17] B. Alric, C. Formosa-Dague, E. Dague, L. Holt, and M. Delarue, Macromolecular crowding limits growth under pressure, *Nat. Phys.* **18**, 411 (2022).
- [18] K. J. Cheung, E. Gabrielson, Z. Werb, and A. J. Ewald, Collective invasion in breast cancer requires a conserved basal epithelial program, *Cell* **155**, 1639 (2013).
- [19] I. Y. Wong, S. Javaid, E. A. Wong, S. Perk, D. A. Haber, M. Toner, and D. Irimia, Collective and individual migration following the epithelial–mesenchymal transition, *Nat. Mater.* **13**, 1063 (2014).
- [20] L. Petitjean, M. Reffay, E. Grasland-Mongrain, M. Poujade, B. Ladoux, A. Buguin, and P. Silberzan, Velocity fields in a collectively migrating epithelium, *Biophys. J.* **98**, 1790 (2010).
- [21] C. Pérez-González, R. Alert, C. Blanch-Mercader, M. Gómez-González, T. Kolodziej, E. Bazellieres, J. Casademunt, and X. Trepat, Active wetting of epithelial tissues, *Nat. Phys.* **15**, 79 (2019).
- [22] A. Elosegui-Artola, A. Gupta, A. J. Najibi, B. R. Seo, R. Garry, C. M. Tringides, I. de Lázaro, M. Darnell, W. Gu, Q. Zhou *et al.*, Matrix viscoelasticity controls spatiotemporal tissue organization, *Nat. Mater.* **22**, 117 (2023).
- [23] G. Y. Ouaknin and P. Z. Bar-Yoseph, Stochastic collective movement of cells and fingering morphology: No maverick cells, *Biophys. J.* **97**, 1811 (2009).
- [24] P. Tracqui, Biophysical models of tumour growth, *Rep. Prog. Phys.* **72**, 056701 (2009).
- [25] M. Basan, J.-F. Joanny, J. Prost, and T. Risler, Undulation instability of epithelial tissues, *Phys. Rev. Lett.* **106**, 158101 (2011).
- [26] P. Ciarletta, Buckling instability in growing tumor spheroids, *Phys. Rev. Lett.* **110**, 158102 (2013).
- [27] M. H. Köpf and L. M. Pismen, A continuum model of epithelial spreading, *Soft Matter* **9**, 3727 (2013).
- [28] F. D. C. Farrell, O. Hallatschek, D. Marenduzzo, and B. Waclaw, Mechanically driven growth of quasi-two-dimensional microbial colonies, *Phys. Rev. Lett.* **111**, 168101 (2013).
- [29] M. J. Bogdan and T. Savin, Fingering instabilities in tissue invasion: An active fluid model, *R. Soc. Open Sci.* **5**, 181579 (2018).
- [30] J. J. Williamson and G. Salbreux, Stability and roughness of interfaces in mechanically regulated tissues, *Phys. Rev. Lett.* **121**, 238102 (2018).
- [31] R. Alert, C. Blanch-Mercader, and J. Casademunt, Active fingering instability in tissue spreading, *Phys. Rev. Lett.* **122**, 088104 (2019).

- [32] Y. Yang and H. Levine, Leader-cell-driven epithelial sheet fingering, *Phys. Biol.* **17**, 046003 (2020).
- [33] C. Trenado, L. L. Bonilla, and A. Martínez-Calvo, Fingering instability in spreading epithelial monolayers: Roles of cell polarisation, substrate friction and contractile stresses, *Soft Matter* **17**, 8276 (2021).
- [34] T. Büscher, A. L. Diez, G. Gompper, and J. Elgeti, Instability and fingering of interfaces in growing tissue, *New J. Phys.* **22**, 083005 (2020).
- [35] K. Vazquez, A. Saraswathibhatla, and J. Notbohm, Effect of substrate stiffness on friction in collective cell migration, *Sci. Rep.* **12**, 2474 (2022).
- [36] T. Pompe, M. Kaufmann, M. Kasimir, S. John, S. Glorius, L. Renner, M. Bobeth, W. Pompe, and C. Werner, Friction-controlled traction force in cell adhesion, *Biophys. J.* **101**, 1863 (2011).
- [37] O. Cochet-Escartin, J. Ranft, P. Silberzan, and P. Marcq, Border forces and friction control epithelial closure dynamics, *Biophys. J.* **106**, 65 (2014).
- [38] S. Tlili, E. Gauquelin, B. Li, O. Cardoso, B. Ladoux, H. Delanoë-Ayari, and F. Graner, Collective cell migration without proliferation: Density determines cell velocity and wave velocity, *R. Soc. Open Sci.* **5**, 172421 (2018).
- [39] T. Wyatt, B. Baum, and G. Charras, A question of time: Tissue adaptation to mechanical forces, *Curr. Opin. Cell Biol.* **38**, 68 (2016).
- [40] M. Basan, T. Risler, J. Joanny, X. SastreGarau, and J. Prost, Homeostatic competition drives tumor growth and metastasis nucleation, *HFSP J.* **3**, 265 (2009).
- [41] J. Ranft, M. Aliee, J. Prost, F. Jülicher, and J.-F. Joanny, Mechanically driven interface propagation in biological tissues, *New J. Phys.* **16**, 035002 (2014).
- [42] P. Recho, J. Ranft, and P. Marcq, One-dimensional collective migration of a proliferating cell monolayer, *Soft Matter* **12**, 2381 (2016).
- [43] See Supplemental Material at <http://link.aps.org/supplemental/10.1103/PhysRevLett.132.018402> for derivation of instability criteria and numerical protocol, which includes Refs. [44–47].
- [44] M. Sussman, P. Smereka, and S. Osher, A level set approach for computing solutions to incompressible two-phase flow, *J. Comput. Phys.* **114**, 146 (1994).
- [45] M. Sussman and E. Fatemi, An efficient, interface-preserving level set redistancing algorithm and its application to interfacial incompressible fluid flow, *SIAM J. Sci. Comput.* **20**, 1165 (1999).
- [46] J. A. Sethian and P. Smereka, Level set methods for fluid interfaces, *Annu. Rev. Fluid Mech.* **35**, 341 (2003).
- [47] S. Osher and J. A. Sethian, Fronts propagating with curvature-dependent speed: Algorithms based on Hamilton-Jacobi formulations, *J. Comput. Phys.* **79**, 12 (1988).
- [48] P. G. Saffman and G. I. Taylor, The penetration of a fluid into a porous medium or Hele-Shaw cell containing a more viscous liquid, *Proc. R. Soc. A* **245**, 312 (1958).
- [49] R. Alert, A. Martínez-Calvo, and S. S. Datta, Cellular sensing governs the stability of chemotactic fronts, *Phys. Rev. Lett.* **128**, 148101 (2022).
- [50] A. Nagilla, R. Prabhakar, and S. Jadhav, Linear stability of an active fluid interface, *Phys. Fluids* **30**, 022109 (2018).
- [51] M. Martin and T. Risler, Viscocapillary instability in cellular spheroids, *New J. Phys.* **23**, 033032 (2021).
- [52] R. Mayor and S. Etienne-Manneville, The front and rear of collective cell migration, *Nat. Rev. Mol. Cell Biol.* **17**, 97 (2016).
- [53] E. Ben-Jacob, I. Cohen, and H. Levine, Cooperative self-organization of microorganisms, *Adv. Phys.* **49**, 395 (2000).
- [54] U. S. Schwarz and S. A. Safran, Physics of adherent cells, *Rev. Mod. Phys.* **85**, 1327 (2013).
- [55] F. Lienert, J. J. Lohmueller, A. Garg, and P. A. Silver, Synthetic biology in mammalian cells: Next generation research tools and therapeutics, *Nat. Rev. Mol. Cell Biol.* **15**, 95 (2014).
- [56] T. E. Angelini, A. C. Dunn, J. M. Urueña, D. J. Dickrell, D. L. Burris, and W. G. Sawyer, Cell friction, *Faraday Discuss.* **156**, 31 (2012).